Proceedings of the
44th IEEE Conference on Decision and Control, and
the European Control Conference 2005
Seville, Spain, December 12-15, 2005

A mode-switching path planner for UAV-assisted search and rescue

Allison Ryan
Department of Mechanical Engineering
University of California, Berkeley
Berkeley, CA, 94720
Email: allison@vehicle.me.berkeley.edu

J. Karl Hedrick
Department of Mechanical Engineering
University of California, Berkeley
Berkeley, CA, 94720
Email: khedrick@me.berkeley.edu

Abstract— **Unmanned aerial vehicles (UAVs) can assist in U.S. Coast Guard maritime search and rescue missions by flying in formation with a manned helicopter while using infrared cameras to search the water for targets. Current search and rescue flight patterns contain abrupt turns that can be achieved by a helicopter but not by a fixed-wing UAV. Therefore, a necessity for UAV-assisted search and rescue is path planning and control that allows a UAV to track a helicopter performing such maneuvers while maintaining the desired sensor coverage and the safety of all aircraft. A feasible path planning algorithm combined with an off the shelf autopilot system is proposed.**

The path planning algorithm consists of four modes, each with an associated domain of application. Each mode is formulated to provide safety and contiguous sensor coverage between the UAV and the helicopter. For each of a series of k corners, the along-track distance between the vehicles is defined as $L(k)$. By representing the path planner as a finite automaton, it is shown that any execution of the system causes the series $\{\mathbf{L(k)}\}$ to converge to zero, thereby resulting in satisfactory tracking.

Simulations were performed with a non-linear UAV model and a commercial autopilot system in the control loop. In these simulations, the desired trajectories were commanded to the autopilot as a series of waypoints. However, the UAV was unable to accurately track the desired trajectories, resulting in oscillatory paths with unpredictable lengths. As a result, the analytic proofs of tracking error convergence and safety do not apply.

I. Introduction

A. Problem description

The U.S. Coast Guard has expressed interest in the use of fixed-wing unmanned aerial vehicles (UAVs) to assist manned helicopters in maritime search and rescue missions. UAVs could increase the rate of area searched using onboard infrared cameras, with no increased human risk, and at little extra cost. A master-slave configuration in which the UAVs track the helicopter without input from its pilot or navigation systems is desired. The helicopter flies in a space-filling curve specified by the Coast Guard operating manual [2]. These curves contain right-angle corners that can be executed by a helicopter but not by a fixed-wing UAV. Specifically, the helicopter is capable of decelerating, turning with a very small radius, and accelerating back to its cruising velocity. The UAV must fly at an essentially constant velocity and has a large minimum turn radius. Thus, UAV-assisted search and rescue requires a control algorithm for a UAV to safely track a helicopter through 90-degree turns while maintaining the desired ground coverage. In this paper, we develop a tracking controller specifically for a single UAV flying on the inside of the expanding square search pattern.

B. Assumptions on mission and hardware

The hardware for UAV-assisted search and rescue will consist of a number of UAVs, an unmodified Coast Guard helicopter, and the UAV central controller, to be located on the helicopter but not interfaced with onboard systems. This means that the entire system will be self-contained, and can be used with any available helicopter at short notice. The UAVs will have minimal onboard equipment, limited to cameras and a waypoint-following autopilot such as the Piccolo system by Cloud Cap Technology [5]. The UAVs' cruising speed will determine the nominal speed of the search pattern. The central controller will include a global positioning system receiver for Kalman Filter estimation of the helicopter's location, velocity, and acceleration [7]. It will also include the command station for the autopilot system, and a laptop computer to run the estimation and control. The tracking algorithm must send feasible trajectories to the UAV autopilot in the form of waypoint commands. Given a feasible trajectory of waypoints, the autopilot will control the UAV's nonlinear dynamics, justifying the use of a kinematic model for the combined autopilot and UAV system, and the phrasing of the helicopter tracking control problem as path planning.

C. Other work

Path planning in two dimensions for a vehicle with turn rate constraints is a well-studied problem, with much development based on Dubins' result [1]. The search and rescue tracking problem differs from Dubins' result in that factors such as collision avoidance and ground coverage must be considered. Also, the goal is to track a moving rather than than fixed target. The adaptation of Dubins' result to tracking a moving target is addressed in [6], where a fixed point in the presence of constant wind is treated as a moving point in the wind-fixed frame. Optimal trajectory tracking using a Dubins model is also discussed in [8]. Previous work specific to the UAV-assisted search and rescue problem addresses tracking of helicopter altitude changes and the effects of redundant sensor coverage due to formation spacing [3]. The contents of this paper are presented in more depth in [4].

0-7803-9568-9/05/$20.00 ©2005 IEEE

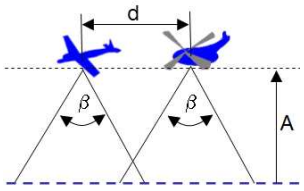

Fig. 1. The distance between the helicopter's and UAV's parallel tracks is determined by their altitude (A) and angles of sensor coverage (β).

D. Paper structure

In section II the helicopter trajectory and the form of the control will be detailed. In section III a specific control will be developed. Analysis of safety and convergence properties, along with simulation results, will be presented in section IV, and conclusions and future work in section V.

II. Problem Formulation

The tracking algorithm will use Kalman Filter estimation of the helicopter's position, velocity, and acceleration to calculate UAV waypoint commands. A waypoint is fixed distance d from the helicopter when its velocity and heading are constant. The distance d between the vehicles' parallel tracks is a function of their altitude A and angle of sensor sweep β, such that sensor coverage at ground-level is maintained with the desired percent redundancy f.

$$d = 2(1-f)A\,tan\left(\frac{\beta}{2}\right) \tag{1}$$

A helicopter following the expanding square search pattern will be modeled as flying at either a constant velocity V or with constant magnitude acceleration a. The pattern consists of straight line segments of increasing length and velocity V, alternated with right turns. A turn is modeled as a constant deceleration to zero velocity, an instantaneous turn, and a constant acceleration back to velocity V. The Kalman Filter will detect the deceleration that begins a turn, as well as estimate V and a to predict the helicopter's position throughout. Turns cannot be simply predicted based on the size of the search pattern due to the uncertainty introduced by the human pilot.

The turn maneuver begins when the helicopter begins to decelerate. At this time, the UAV is located a distance L behind the helicopter, measured along-track as shown in fig. 2. $L(k)$ is defined as this distance, measured at the beginning of the turn maneuver with index k in a series. The end of the turn maneuver can be defined in space by choosing a finish line perpendicular to the helicopter path at which the helicopter and UAV have constant parallel headings and speeds.

The progression of $\{L(k)\}$ is determined only by the UAV's path during the series of turn maneuvers because the UAV's and helicopter's relative positions are fixed when not turning. The UAV will complete the turn maneuver in T_u seconds, and the helicopter in T_h seconds. $L(k+1)$ can now be written as a function of T_u and T_h, where T_u will depend on $L(k)$ and the UAV's path. Any variation from a

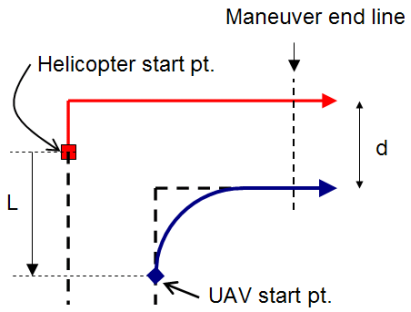

Fig. 2. A representative turn maneuver showing UAV and helicopter positions at start, and common finish line.

vehicle's expected route or velocity that takes place between turn maneuvers will appear as a disturbance, $\Delta(k)$.

$$L(k+1) = (T_u - T_h)V + \Delta(k) \tag{2}$$

The series $\{L(k)\}$ parameterizes the UAV's tracking error through a series of turns, evaluating the two-dimensional continuous time tracking problem in terms of the single discretely evolving variable, L. A path planning law can now be evaluated based on the resulting convergence properties of $\{L(k)\}$ and the sensor coverage provided throughout the turn. During a corner maneuver, the control law takes the form of a set of path planning rules, $\{T_i\}$. A particular path rule T_i is implemented when $L(k)$ falls within the associated domain, D_i, and determines $L(k+1)$ according to the progression function F_i. Implementation of path rule T_i results in a certain UAV path length, and corresponding time T_u. Therefore T_i determines $L(k+1)$ as in equation (2), or more generally as follows.

$$L(k+1) = F_i(L(k)) + \Delta(k), \qquad L(k) \in D_i \tag{3}$$

The interaction of the set of path rules can be represented as a finite automaton with discrete states $\{T_i\}$ and invariants $\{D_i\}$. A transition from T_i to T_j is enabled when $L(k) \in T_i$ and $F_i(L(k)) \in T_j$. A transition is made at each discrete time step, and because $\{D_i\}$ partitions the space of $L(k)$, exactly one transition will be enabled and the execution will be deterministic.

III. Solution: A Set of Four Path Rules

The following four path planning rules form a solution to the search and rescue tracking problem. They guarantee convergence of $\{L(k)\}$ and safe separation between the UAV and helicopter, and are formulated to provide ground coverage. Convergence is based on a particular (convergent) path rule that causes the series $\{\mathrm{L(k)}\}$ to converge geometrically to zero after the execution enters that path rule's domain. The other path planning rules ensure that for any initial condition, the execution enters the domain of the convergent path rule in a small number of steps.

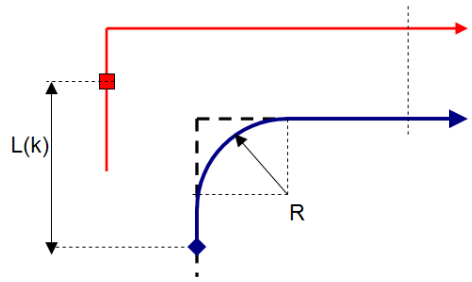

Fig. 3. Cutting the corner (T_1) reduces large lag.

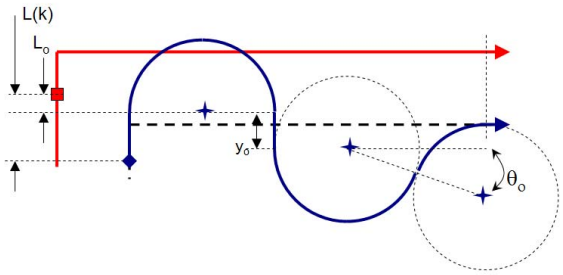

Fig. 4. The fixed curve (T_2) causes constant reduction in lag and provides better sensor coverage than the convergent rule would over this domain.

1) Cut Corner Path: For large values of $L(k)$, the UAV can round off the inside of the corner, resulting in $L(k+1)$ greatly reduced (fig. 3). The domain is calculated geometrically such that $L(k+1) \geq min\, D_3$, where D_3 is the domain of the convergent path rule. This prevents the existence of a cycle in the transition graph.

$$\begin{aligned} D_1 &= \left\{ L(k) : \frac{V^2}{2a} + 2d + \left(2 - \frac{\pi}{2}\right) R \right\} \\ F_1 &= L(k) - \frac{V^2}{a} - 2d + \left(\frac{\pi}{2} - 2\right) R \end{aligned} \tag{4}$$

2) Fixed Curve Path: The fixed curve path rule is a variation of the convergent rule, where the path is modified to keep the UAV closer to the helicopter for better ground coverage. It can be seen in the following section that the second arc in the convergent path rule moves farther from the helicopter's track as $L(k)$ increases, which would eventually result in a coverage gap for large $L(k)$. Instead, for $L(k)$ equal to L_0, the arcs are fixed, resulting in constants y_0 and θ_0 for the fixed curve path rule. When $L(k)$ is greater than L_0, the UAV begins to turn the corner a distance L_0 behind the helicopter's new path instead of immediately as it would in path rule three.

$$\begin{aligned} D_2 &= \left\{ L(k) : L_0 \leq L(k) \leq \frac{V^2}{2a} + 2d + \left(2 - \frac{\pi}{2}\right) R \right\} \\ F_2 &= (c-1)L_0 + L(k) \\ L_0 &= \frac{1}{c+1}\left[\left(\frac{5\pi}{2} - 4\right) R - \frac{2V^2}{a}\right] \\ c &\quad \textit{chosen by designer in } T_3 \end{aligned} \tag{5}$$

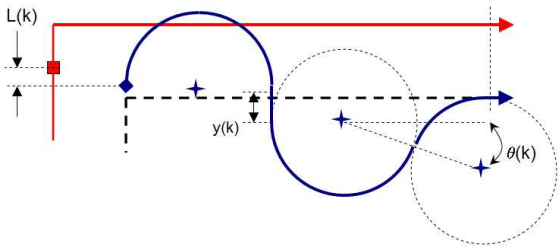

Fig. 5. The convergent rule (T_3) causes {L(k)} to converge exponentially to zero.

3) Convergent Path: The convergent path consists of a half-circle, a straight segment, and two tangent arcs (fig. 5). The angle θ decreases as the second arc is shifted farther from the UAV's desired track. This path rule is defined on a domain in which the UAV starts the turn on the near side of the helicopter's new path and angle θ will be positive, i.e., the path consists of just one intermediate straight segment. $\theta(k)$ is a function of the length $y(k)$ of the straight segment, which is selected so that $\{L(k)\}$ converges geometrically to zero (6) at a rate c selected by the designer.

$$L(k+1) = c\, L(k), \quad c \in (0,1) \tag{6}$$

$$\begin{aligned} &D_3 = \\ &\left\{ L(k) : \tfrac{-V^2}{2a} < L(k) < \tfrac{1}{c+1}\left[\left(\tfrac{5\pi}{2} - 4\right) R - \tfrac{2V^2}{a}\right] \right\} \\ &L(k+1) = \\ &\left(\tfrac{5\pi}{2} - 2\theta(k) - 3 - 2\cos\theta(k)\right) R + y(k) - d - \tfrac{3V^2}{2a} \\ &\theta(k) = \arcsin\left(\tfrac{R+d-L(k)-y(k)-\frac{V^2}{2a}}{2R}\right) \end{aligned} \tag{7}$$

Eqn. 7 cannot be solved explicitly for the desired $y(k)$ that will produce $L(k+1)$ as in 6. However, by fixing $L(k)$, $L(k+1)$ can be approximated very accurately as a linear function of $y(k)$ and replaced by its first order Taylor expansion. The function $L(k+1)$ is linearized at the point $(y_o, L(k))$. The selection of y_o can be made a priori because its effect is linear over the entire range.

$$\begin{aligned} L(k+1) &= f(L(k), y(k)) \\ f(L(k), y(k)) &\approx f(L(k), y_o) + \left.\frac{\partial f}{\partial y}\right|_{y=y_o} (y - y_o) \\ \left.\frac{\partial f}{\partial y}\right|_{y=y_o} &= 1 + \frac{1 - \sin\theta_o}{\sqrt{1 - \left(\frac{R+d-L(k)-\frac{V^2}{2a}-y_o}{2R}\right)^2}} \end{aligned} \tag{8}$$

The distance $y(k)$ can now be selected based on the approximation of its relation with $L(k+1)$.

$$y(k) = y_o + \frac{c\, L(k) - f(L(k), y_o)}{\left.\frac{\partial f}{\partial y}\right|_{y=y_o}} \tag{9}$$

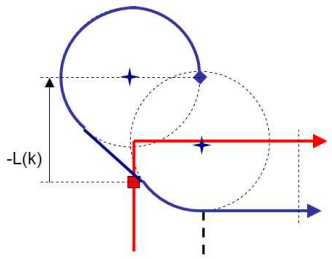

Fig. 6. The outside loop path (T_4) greatly increases lag when UAV begins a turn ahead of helicopter.

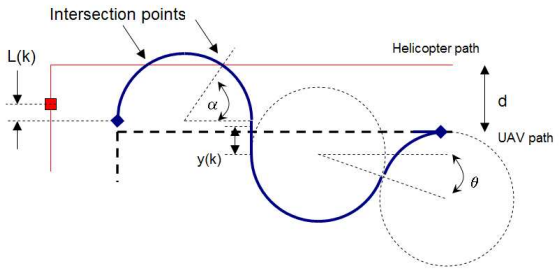

Fig. 7. Two intersection points for path rule 3, located at angles α and $\pi - \alpha$.

4) Outside Loop Path: If the UAV begins the turn maneuver ahead of the helicopter's new path, as shown in fig. 6, its safe path is to loop back behind the helicopter. This leads to large $L(k+1)$, causing the UAV to lag behind the helicopter in the next turn.

$$D_4 = \left\{ L(k) : L(k) < \tfrac{-V^2}{2a} \right\}$$
$$L(k+1) = \tfrac{3\pi}{2} R - \tfrac{3V^2}{2a} - d + \sqrt{R^2 + \left(L(k) + \tfrac{V^2}{2a} - d + R \right)^2} \quad (10)$$

IV. Analysis and Simulation

Assuming that the helicopter executes the square spiral search pattern, and that the UAV perfectly tracks the path assigned by the active path rule, the progression of $\{L(k)\}$ can be modeled as in (3) without accounting for the system's continuous-time dynamics. This type of simulation was used to verify the analysis of convergence properties. A more accurate simulation can be produced using a non-linear six degree of freedom UAV model controlled by a Piccolo autopilot. This is referred to as a hardware in the loop (HIL) simulation because the autopilot hardware is in the control loop. In this case, the Kalman Filter and mode-switching path planner are implemented using C++ and send waypoint commands to the Piccolo autopilot. This environment is very high fidelity because only the UAV's flight dynamics are simulated; all other UAV systems are as they would be in application.

The following parameter values were used for all simulations. The UAV dynamics V and R are estimated from the SigRascal experimental platform at the University of California, Berkeley [5], which will be used for future field testing. The separation d is calculated using (1) and an altitude suggested in U.S. Coast Guard documentation [2]. This altitude also ensures that a human-sized target will occupy a sufficient number of pixels on an application-typical infrared camera. The autopilot system receives GPS updates at 1 Hz.

V = 20 $\frac{m}{s}$	UAV and helicopter nominal velocity
R = 100 m	UAV minimum turn radius
a = 2.5 $\frac{m}{s^2}$	helicopter acceleration
A = 150 m	altitude
d = 250 m	desired separation between UAV and helicopter

The mathematical properties of the four path planning rules can be used to show that the aircraft will maintain a safe separation distance and that the helicopter tracking error will converge to zero. These analytical properties are then compared to the results of HIL simluation.

A. Collision avoidance conditions

Each of the path rules proposed in the previous section provides a safe path for the UAV. Path rule one is not addressed because the helicopter and UAV do not cross paths. Under path rule two, the UAV begins its first turn at distance L_o from the helicopter's initial position. If L_0 satisfies (11), the UAV will not cross the helicopter's path.

$$L_o > R - \frac{V^2}{2a} \quad (11)$$

Substituting for L_o (5) leads to the following condition for the safety of this trajectory. If this is not satisfied, the UAV will cross the helicopter's path, and there is a chance of collision. Recall that c was chosen by the designer as the convergence rate of path rule three, and is between zero and one.

$$\frac{V^2}{2aR} > \frac{\frac{5\pi}{2} - 5 - c}{3 - c} \quad (12)$$

Following path rule three, the UAV immediately begins turning in an arc that may cross the helicopter's path twice, as shown in fig. 7. The intersection points are located at angles α and $\pi - \alpha$ along the arc, and the UAV and helicopter pass through the points with separations of T_1 and T_2 seconds. The worst case time differences for the two vehicles passing through these points are as follows.

$$minT_1 = \frac{3V}{2a} + \frac{d + R - R\pi}{V} + \frac{R}{V} \min_{0 \le \alpha \le \pi/2} \{\cos\alpha + \alpha\}$$

$$minT_2 = \frac{3V}{2a} + \frac{d + R}{V} - \frac{R}{V} \max_{0 \le \alpha \le \pi/2} \{\cos\alpha + \alpha\}$$

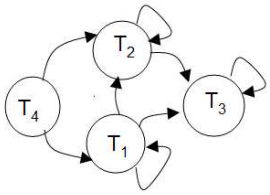

Fig. 8. Possible transitions between domains of path rules

The designer will likely specify some minimum clearance time T_d to ensure a factor of safety, resulting in the following conservative requirement on V, a, and R after substituting for the appropriate limits. This requirement and (12) are both satisfied over a range of parameters including the simulation values.

$$\frac{3V}{2a} + \frac{d-R}{V} > T_d \tag{13}$$

Although the UAV's and helicopter's paths intersect once under rule four, the helicopter passes through the intersection point almost immediately and the UAV passes through it only after completing a minimum turn radius loop (fig. 6), so there is no danger of collision.

B. Convergence properties

Recall that after $\{L(k)\}$ converges to zero, the UAV will begin each corner at its desired location ($L = 0$) if there is no disturbance. We show that this will occur for any initial condition $L(1)$, and that the required number of corners before convergence is a bounded function of $L(1)$.

The convergence guarantee of the combination of path rules is based on the convergent rule T_3, which causes $\{L(k)\}$ to converge geometrically to zero. Thus, showing that all trajectories enter D_3 is equivalent to proving convergence for the system. Because in the absence of disturbances, $L(k+1)$ depends only on $L(k)$, the range R_i of possible $L(k+1)$ resulting from each path rule can easily be determined. F_1, F_2, and F_3 are all linear in $L(k)$ with positive slope, and F_4 decreases monotonically with $L(k)$ over its range. Therefore, the extrema of the ranges occur at the extrema of the domains of each path rule. Comparing the extrema of the ranges to the extrema of the domains allows the possible transitions between path rules to be enumerated as shown in fig. 8.

It can be seen from fig. 8 that all paths either lead to the convergent domain or remain in a cycle on T_1 or T_2. Therefore, by showing that the cycles on T_1 and T_2 can occur only a finite number of times, we show that $\{L(k)\}$ enters D_3 in finite time. This is easily shown by the fact that for each of T_1 and T_2, $L(k+1)$ decreases by a positive constant C_i. D_1 and D_2 are both lower bounded, so the maximum number of executions (N_i) of either loop is bounded.

$$\begin{aligned} N_1 &\leq (L(1) - min\{D_1\})/C_1 \\ N_2 &\leq (max\ D_2 - min\{D_2\})/C_2 \end{aligned} \tag{14}$$

Thus, for any initial condition, $\{L(k)\}$ reaches D_3 in fewer than $3 + N_1 + N_2$ steps, and then converges exponentially to zero in the absence of disturbance. When the UAV or helicopter is allowed to deviate from its expected trajectory and introduce a disturbance, convergence can be ensured to a limited extent. Because the disturbance is not filtered through plant or controller dynamics, it cannot be directly attenuated. Therefore, a constant disturbance will result in steady state error. However, disturbances will not be amplified, and any single large disturbance has the same effect as restarting the system from a new initial condition, so convergence properties hold.

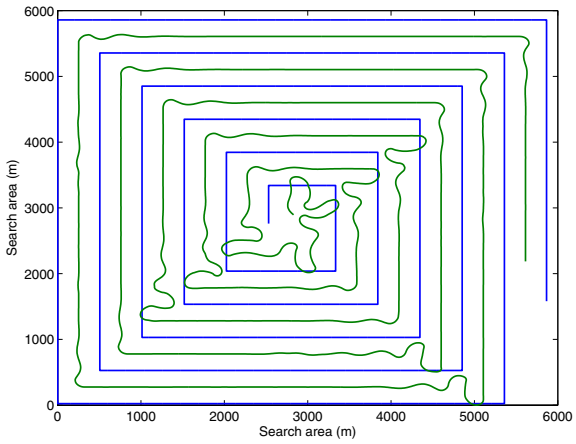

Fig. 9. Aircraft paths from hardware in the loop simulation. Note the curved UAV path resulting from the mode-switching search and rescue controller.

TABLE I

THE REDUNDANCY, OR OVERLAP IN THE SENSOR FOOTPRINTS OF THE UAV AND HELICOPTER, AFFECTS THE PERCENTAGE OF SENSOR COVERAGE OVER THE SEARCHED AREA.

percent redundancy	percent coverage
0	99.65
5	99.63
10	99.83

C. Simulation Results

Fig. 9 shows the helicopter and UAV paths from a typical HIL simulation. The percent sensor coverage of the search area is measured by plotting appropriately sized sensor footprints over the UAV's and helicopter's paths.

A single helicopter perfectly tracking a space filling curve can provide perfect sensor coverage of the ground. UAV assistance decreases the required density of the helicopter's space-filling curve, and therefore allows faster search rates. However, when the UAV varies from the ideal space filling curve, gaps in sensor coverage may result. This effect also depends on the degree of redundancy in the formation spacing, represented by f in (1). Increasing the redundancy reduces both the gaps in sensor coverage and the search speed. This tradeoff is examined for simulations with 0, 5, and 10 percent redundancy in the formation spacing and the results are shown in table I.

The sensor coverage results all fall within a very small range, meaning that it is difficult to conclude differences be-

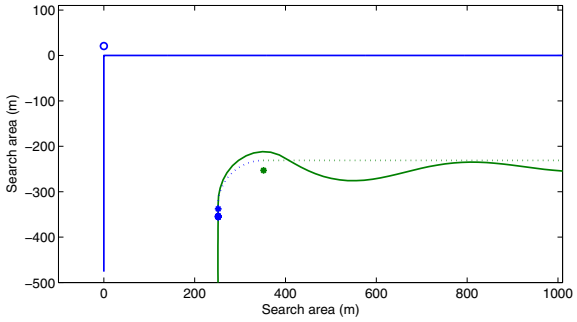

Fig. 10. Helicopter and UAV paths are plotted as solid lines beginning from the bottom of the figure. The UAV's desired path is a broken line, and its commanded waypoints are shown. The circle shows the controller's initial estimate of where the helicopter will turn.

tween the three tests. All tests provided satisfactory coverage, and generally support the prediction that greater redundancy will provide greater coverage.

It can be seen that the simulated UAV path from fig. 9 is more oscillatory than the trajectories designed in section III. All simulations showed similar results. The oscillations cause the UAV's path length around each corner to be longer than desired, meaning that the collision avoidance and tracking error properties can no longer be guaranteed because they depend on control of path length.

Fig. 10 shows a representative corner from the simulation in fig. 9 where the controller commands the UAV to cut the corner. The helicopter's and UAV's paths are shown as solid lines, and the UAV's expected path is shown broken. The circle above the corner in the helicopter's path shows the controller's estimate of where the corner will occur, estimated when deceleration is first detected. The estimation error is caused by slight underestimation of the helicopter's deceleration and delay in detecting it. This estimate is corrected before the UAV begins its maneuver, and so has no effect in this case. However, in some cases when $L(k)$ is small and the UAV's and helicopter's paths intersect, this estimation error leads to unacceptable clearance distance between the two vehicles.

The markers on the UAV's path show the commanded endpoints of the arc. The marker at the beginning of the arc shifts when the estimate of the helicopter's corner is corrected. Note that the UAV does not achieve the necessary turn rate to reach the commanded end point. This is due to delay in beginning the turn and overestimation of the UAV's maximum turn rate. As a result, the UAV overshoots its desired path. This type of overshoot also leads to near-collisions in some cases.

The UAV's failure to track the desired trajectory added 300 to 550 meters to its path length in HIL simulations. As a result, the transition diagram in fig. 8 is no longer correct, and the tracking error does not converge. In the simulation shown in fig. 9, the UAV alternates between corners of type one and two. The convergence properties developed previously depend on a transition to path rule three. The additional 300 to 500 meters in path length cause a transition back to path rule one instead, thereby creating a cycle between path rules one and two that causes $\{L(k\}$ to remain in the range of approximately 400 to 1000 meters.

V. Conclusions and Future Work

UAV-assisted search and rescue in the existing Coast Guard framework requires a tracking and formation flight algorithm that provides reliable ground coverage and ensures the safety of all aircraft. By assuming that an onboard autopilot is capable of tracking a feasible waypoint path, this problem is reduced from controller design to path planning. In this case we consider the path planning for a single UAV flying on the inside of a spiral pattern. The solution consists of a set of four path planning rules, which combine to provide safety and convergence guarantees.

The path rules were selected to keep the UAV as close as possible to its nominal trajectory within the constraints of vehicle kinematics, collision avoidance, and steady state tracking. In hardware in the loop simulation, unmodeled delays and estimation error caused the UAV to deviate from the desired trajectories. These deviations cause unpredictable path lengths, thereby negating the path-dependent guarantees of collision avoidance and tracking error convergence. These issues may be resolvable by using a more powerful trajectory tracking controller rather than parameterizing the desired path using a small number of waypoints.

The complete solution to UAV-assisted search and rescue must also include high-level control for tasks such as formation reconfiguration, recognition and tracking of detected objects. An independent collision avoidance control should also be included.

References

[1] L.E. Dubins, "On Curves of minimal length with a constraint on average curvature and with prescribed initial and terminal positions and tangents", *American Journal of Mathematics*. 79:497-516. 1976

[2] *U.S. Coast Guard Addendum to the United States National SAR Supplement* (CGADD), COMDTINST M16130.2C, Chapter 3 and Appendix H, available at: http://www.uscg.mil/hq/g-o/g-opr/manuals.htm

[3] Anna Williams, *Search and rescue augmentation using unmanned aircraft*, Masters Thesis, UC Berkeley, 2004.

[4] Allison Ryan, *A mode-switching path planner for UAV-assisted search and rescue*, Masters Thesis, UC Berkeley, 2005.

[5] A. Ryan, M. Zennaro, A.S. Howell, R. Sengupta, and J.K. Hedrick, "An Overview of Emerging Results in Cooperative UAV Control", *Proceedings of the IEEE Conference on Decision and Control*, Dec. 2004.

[6] T. McGee, S. Spry, and J.K. Hedrick, "Optimal path planning for an aircraft with a bounded turn rate in the presence of a constant wind", submiited to the *AIAA Conference on Guidance, Navigation, and Control*, August 2005.

[7] R.E. Kalman, "A new approach to linear filtering and prediction problems", *Trans. of the ASME Journal of Basic Engineering*, Vol. 82, 1960.

[8] P. Soueres, A. Balluchi, A. Bicchi, "Optimal feedback control for route tracking with a bounded-curvature vehicle", *Proceedings of the IEEE International Conference on Robotics and Automation*, April 2000.